ERDC/CERL TR-01-39

Engineer Research and Development Center

US Army Corps of Engineers®
Engineer Research and Development Center

Spatial and Temporal Prediction and Uncertainty Analysis of Rainfall Erosivity for the Revised Universal Soil Loss Equation

Guangxing Wang, George Gertner, Vivek Singh, Svetlana Shinkareva, Pablo Parysow, and Alan B. Anderson

May 2001

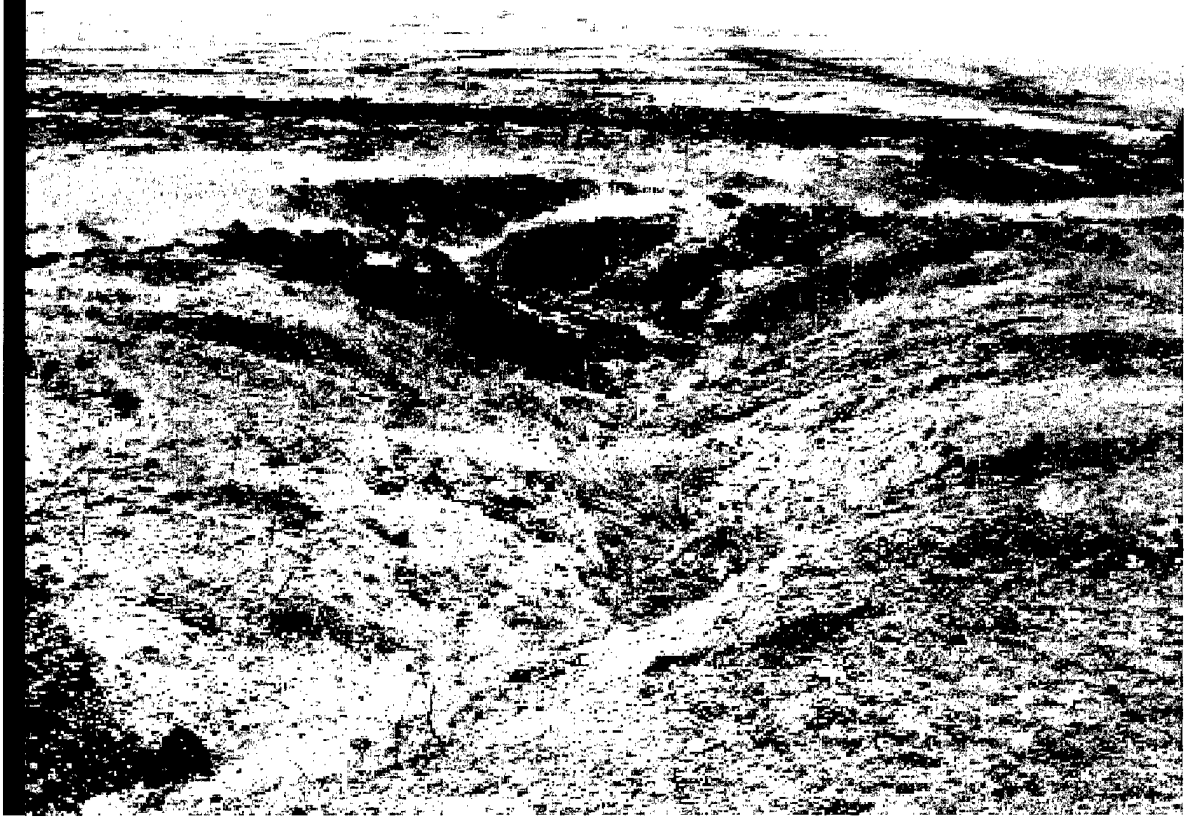

Foreword

This study was conducted for the Strategic Environmental Research and Development Program (SERDP) Office under Funding Authorization Document (FAD) 0400-99-8141-08, Work Unit EE9, "Error and Uncertainty for Ecological Modeling and Simulation" (CS-1096). The technical monitor was Dr. Robert W. Holst, Compliance and Conservation Program Manager, SERDP. Bradley P. Smith is the Executive Director, SERDP.

The work was performed by the Ecological Processes Branch (CN-N) of the Installations Division (CN), Construction Engineering Research Laboratory (CERL). The CERL Principal Investigator was Alan Anderson. Part of the work was done by Dr. Guangxing Wang, Dr. George Gertner, Dr. Vivek Singh, and Dr. Svetlana Shinkareva of the University of Illinois and by Dr. Pablo Parysow of Northern Arizona University, Flagstaff, AZ. The technical editor was Linda L. Wheatley, Information Technology Laboratory. Stephen E. Hodapp is Chief, CN-N, and Dr. John T. Bandy is Chief, CN. The Technical Director is Dr. William D. Severinghaus, CVT. The Acting Director of CERL is William D. Goran.

CERL is an element of the U.S. Army Engineer Research and Development Center (ERDC), U.S. Army Corps of Engineers. The Director of ERDC is Dr. James R. Houston and the Commander is COL James S. Weller, EN.

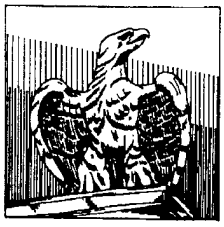

Contents

List of Figures, Tables, and Equations

Figures

Tables

Equations

1 Introduction

Background

Integrated Training Area Management (ITAM) Program

The Department of Defense (DoD) is responsible for administering more than 25 million acres of federally owned land in the United States (Public Land Law Review Commission 1970), making it the fifth largest Federal land management agency. A major objective of the ITAM program — the Army's program for managing training land — has been to develop a method for estimating training land carrying capacity. The Office of the Deputy Chief of Staff for Operations and Plans (ODCSOPS) defines training land carrying capacity as the amount of training that a given parcel of land can accommodate in a sustainable manner, based on a balance of use, condition, and maintenance practices. ODCSOPS has sponsored the Army Training and Testing Area Carrying Capacity (ATTACC) program to estimate this training land carrying capacity.

ATTACC Methodology

The ATTACC methodology is used to estimate training and testing land carrying capacity. It is also used to determine land rehabilitation and maintenance costs associated with land-based training and other land uses. The *ATTACC Handbook* (U.S. Army Environmental Center [AEC] 1999), Army Regulation (AR) 350-4, and Department of the Army Pamphlet (DA PAM) 350-4 document the standard operating procedures for implementing ATTACC.

The Evaluation of Land Value Study (ELVS) methodology, a precursor to ATTACC, was an initiative sponsored by ODCSOPS and the Assistant Secretary of the Army (Installations, Logistics, and Environment) [ASA (IL&E)]. ELVS was developed to estimate training land carrying capacity and the cost of land rehabilitation and maintenance associated with land-based training (Anderson et al. 1996). The ELVS methodology quantified training land condition in terms

of Maneuver Impact Miles based on mileage projections from the Battalion Level Training Model and training event and vehicle impact severity factors. It also used a modification of the Revised Universal Soil Loss Equation (RUSLE)* to estimate land condition in terms of erosion status as a function of the training load. Land rehabilitation and maintenance costs were obtained from existing installation records and regional cost estimates of particular practices. The ELVS methodology was applied to eight pacing units in heavy maneuver training at Fort Hood, TX, and the Combat Maneuver Training Center, Hohenfels, Germany.

The ELVS methodology was expanded, updated, and redesignated as ATTACC. The ATTACC methodology extends the ELVS initiative to include all types of Army units (including unique combat units), Army service schools, Reserve Component (RC) units, and RC-unique requirements. The ITAM program is integrating the ATTACC methodology into the Army's Weapon System Cost Factor Development Program and providing tools for installation personnel to use to develop local requirements and impacts analysis. Portions of the ATTACC methodology were incorporated into the Range Facilities Management and Support System to provide installation schedulers with a means to estimate training load during scheduling activities.

ATTACC-Related Army User Requirements

Documentation of the Army's environmental technology requirements has been an iterative process that began with a series of meetings in 1993 and the Office of the Directorate of Environmental Programs' (ODEP's) publication, *U.S. Army Environmental Requirements and Needs*, which describes the critical research, development, test, and evaluation needs for accomplishing the Army's mission with the least impact or threat to the environment. These Army-level requirements were reviewed for their effect on readiness, quality of life, the environment, and the timeliness needed for the Army to maintain compliance with environmental regulations. All major commands, major subcommands, ODCSOPS, and the Office of the Deputy Chief of Staff for Logistics were involved in establishing the prioritized and validated list of the Army's environmental technology requirements.

* Described in Chapter 2.

Land Capacity and Characterization is the third priority conservation user requirement on the Army's list. This user requirement defines the Army's need to estimate training land carrying capacity, and describes the ATTACC methodology as a means to provide land managers with scientifically based information to support sound decisionmaking. However, this user requirement also defines the current version of ATTACC as limited in its ability to provide the most accurate information for decisionmaking. This limitation is related to the accuracy of input data and a simplistic characterization of the three components of the model. The user requirement identifies research and development required to improve the accuracy of ATTACC.

The *Land Capacity and Characterization* user requirement identified 28 exit criteria. Each criterion defines a specific product required to address a specific aspect of the overall requirement. Two exit criteria address the temporal and spatial uncertainty of model inputs and predictions. These exit criteria are:

1. Develop a protocol, tool(s), and/or factors for installation-level use that reflect a probable range of results in the ATTACC methodology.
2. Develop a protocol, tool(s), and/or factors for installation-level use that improve spatial results from ATTACC.

ATTACC Sensitivity Analysis

A sensitivity analysis evaluates the magnitude of changes in a model's output as a function of changes in the input parameter values. Moreover, a sensitivity analysis of a model's responses to variations in input values can be used to determine the relative importance of individual input values. Results of a sensitivity analysis are used to prioritize data acquisition and model development efforts.

A sensitivity analysis of ATTACC methodology (Anderson 1999) has found the methodology to be sensitive to changes in the climatic factor of the RUSLE. This finding implies that improvements to the R factor portion of the methodology can result in an overall improvement in model accuracy. The R factor will be described in the next chapter.

Objectives

The purpose of this research was to determine a mapping strategy for spatial and temporal prediction and uncertainty analysis of the rainfall and runoff erosivity R factor. The strategy, presented in this report, is based on sequential

Gaussian simulation. Its key is modeling spatial and temporal variability of the R factor using semi-variograms and deriving expected estimates and their variances at any location and time. The temporal variability of this factor is investigated by annual, seasonal, and half-month time series simulation. The specific objective was to compare uncertainty using the simulation and traditional isoerodent maps. The strategy is illustrated in a case study in which no rainfall data were available for the area of interest. The study area was expanded to include a larger area where rainfall data were available to develop prediction models. From the larger area, data for the area of interest on Fort Hood was then extracted.

Approach

The temporal and spatial variability of the RUSLE R factor was first modeled using semi-variograms in geostatistics. Sequential Gaussian simulation was then used for uncertainty analysis. A case study illustrates the strategy.

Previous applications traditionally used R factor values obtained from empirical isoerodent maps that were assumed to be constant over time and space. R factor values using the proposed strategy were compared to the traditional approach to demonstrate differences between the two approaches.

Scope

The project presented in this report is part of a larger initiative titled *Error and Uncertainty Analysis for Ecological Modeling and Simulation.* The objectives of the larger effort are to develop a general methodology and framework for spatial and temporal modeling, simulation, and uncertainty analysis of natural resource, ecological, and environmental systems. Furthermore, various sources of errors such as measurement errors, sampling errors, model errors, expert knowledge, uncertainty, etc., are being identified, their propagation modeled and error budgets developed in order to provide management guidelines. The case study selected for this overall effort is the ATTACC methodology. The results presented in this report are for one factor of the RUSLE, a central component of ATTACC. Similar efforts have been initiated for other components of the RUSLE and ATTACC models. Results of these efforts are being reported elsewhere. The information provided here refers to the ATTACC methodology as described in the *ATTACC Handbook* (AEC 1999).

Mode of Technology Transfer

This strategy for RUSLE R factor prediction and uncertainty analysis will be provided directly to Army personnel responsible for ATTACC implementation. The information is also provided to organizations responsible for developing and refining the ATTACC methodology.

Units of Weight and Measure

Some U.S. standard units of measure are used in this report. A table of conversion factors for Standard International (SI) units is provided below.

SI conversion factors		
1 in.	=	2.54 cm
1 ft	=	0.305 m
1 lb	=	0.453 kg

2 Approaches for Derivation of R Factor Values

The RUSLE is widely used to predict average annual soil loss for specific locations. RUSLE is an empirical model in which soil loss depends on the factors of rainfall erosivity (R), soil erodibility (K), slope steepness (S), slope length (L), cover management (C), and support practice (P) (Renard et al. 1997).

Soil erosion is greatly influenced by the intensity and duration of precipitation events and by the amount and rate of the resulting runoff. The R factor is a quantitative expression of the erosivity of local average annual precipitation and runoff. R factor values are derived from research data (Wischmeier 1959; Wischmeier and Smith 1958). Erosivity index (EI) values are estimated for each precipitation event. The annual rainfall and runoff erosivity factor is the sum of the EI values for all rain events in a year. Larger rainfall and runoff erosivity factor values indicate climatic conditions with higher potential for soil loss.

Isoerodent maps developed using historical data (frequently a 30-year period) are widely used to estimate a rainfall EI for a specific area (Renard et al. 1997). Linear interpolation is used to estimate EI between the contour lines of the isoerodent maps. This approach assumes that the rainfall erosivity factor is linear over space and constant over time. As suggested by McGregor, Mutchler, and Bowie (1980), this assumption may not be true in all cases. For example, global climate change might result in a change in the frequency of annual precipitation and thus in a change of rainfall EI.

Although spatially explicit EI can be derived by linear interpolation, a constant value for an area is usually applied. This application may lead to spatial prediction smoothing and unaccounted uncertainty related to this smoothing. Furthermore, uncertainty of the rainfall EI from the isoerodent maps is usually unknown. Additionally, calculation of R factor values for new locations and areas is laborious and requires long-term rainfall intensity data.

An alternate method is to use a simple linear regression between the rainfall EI and average annual precipitation data (Bollinne et al. 1980). Mikhailova et al. (1997) further developed a regression of the rainfall EI as a function of average

annual precipitation and elevation. Elevation was found to be highly significant in predicting rainfall EI. Goovaerts (1999) presented a geostatistical method for this purpose, where a digital elevation model is incorporated into mapping annual and monthly erosivity values. His study suggested that geostatistical methods were promising for monitoring and mapping rainfall and runoff erosivity. Geostatistical methods are divided into kriging and simulation algorithms, which are extensively applied in natural resource and environmental sciences.

Kriging is a generalized least-squares algorithm minimizing the magnitude of the error variance with unbiased estimates, and can be used for making spatial prediction at unknown locations based on measurements from known locations. Modeling prediction uncertainty is based on semi-variograms measuring the spatial variability of the data. Kriging estimates are smoothed and are best in local prediction; however, kriging variances depend only on the data configuration and not on the actual observed data, and thus do not adequately reflect uncertainty. Examples of kriging include the interpolation of heavy metal concentrations in a contaminated site using three kriging estimators by Juang and Lee (1998) and the work of Rogowski and Wolf (1994) on variability of soil map unit delineation using a kriging method.

The other geostatistical approach uses spatial simulation techniques whereby the conditional distributions are developed according to collected data sets. From these distributions the values of the stochastic variable at unknown locations are drawn at random. Once values at all the unknown locations are simulated, a realization of the stochastic variable is developed. After many realizations, the set of alternative realizations provides a visual and quantitative measure (actually a model) of spatial uncertainty (Wang et al. 2000; Goovaerts 1997). The expected estimates and various uncertainty measures such as conditional variances and probability maps can be derived from the realizations. The error variances depend not only on data configuration, but also on the data themselves, thus implying global uncertainty. The most commonly used technique is sequential Gaussian simulation.

3 Study Area, Data Set, and Rainfall R Factor

Fort Hood, the study area for this research, occupies 87,890 hectares (ha) (Nakata 1987) in the central Texas counties of Bell and Coryell. Fort Hood's climate is characterized by long, hot summers and short, mild winters. Average temperatures range from a low of about 8 °C in January to a high of 29 °C in July. Average annual precipitation is 81 cm. Table 1 shows average monthly and maximum rainfall values for Fort Hood.

Elevation at Fort Hood ranges from 180 to 375 m above sea level with 90 percent of the area below 260 m. Most slopes are in the 2 to 5 percent range, with slopes in excess of 45 percent occurring as bluffs along the flood plain and as the sides of slopes on the hills. Fort Hood lies in the Cross Timbers and Prairies vegetation area (Gould 1975), which is normally composed of oak woodlands with grass undergrowth. Soil cover is generally shallow to moderately deep and clayey, underlain by limestone bedrock.

Based on traditional isoerodent maps, the annual R factor value for Fort Hood is a constant 270 (Renard et al. 1997). No rainfall observation stations were within the study area, however. It was necessary, therefore, to use data from rainfall observation stations in the surrounding area. The 247 rainfall stations ultimately used were located in Texas and the surrounding states of Arkansas, Colorado, Kansas, Louisiana, New Mexico, and Oklahoma. Figure 1 shows the geographical location of these stations. Out of the 247 stations, 29 were randomly sampled and used as a validation data set. The remaining 218 stations were used to develop the spatial models.

Table 1. Average annual climatic data for Fort Hood, TX.

Month	Average Monthly Rainfall (cm)	Maximum 24-hr Rainfall (cm)
January	5.1	5.8
February	5.6	6.3
March	5.6	5.1
April	9.4	4.3
May	11.4	22.6
June	8.4	8.6
July	4.6	4.1
August	7.1	6.1
September	8.9	12.2
October	9.7	7.9
November	5.1	5.6
December	4.3	3.8

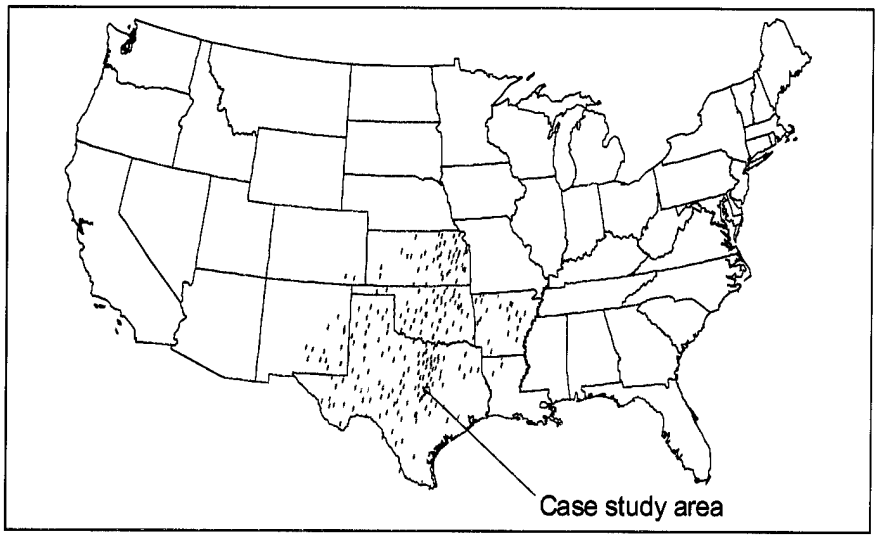

Figure 1. Spatial location of rainfall stations in large area.

The R factor values for rainfall erosivity were calculated for each rainfall station by a method developed by a research team headed by Hollinger.* This team is in the process of calculating R factor values on a half-month basis across the entire United States. An annual R factor value is the sum of rainfall EI for all rain events within a year. If a rainstorm produces less than 0.5 in. of rain during a period of 6 hours (Wischmeier and Smith 1978), the EI of the rainstorm is obtained by multiplying kinetic energy of the rain with 30-minute maximum rain intensity. Equation 1 was used to calculate the energy contained in the volume of rain:

Equation 1. Erosivity equation.

$$E = 0.29 \times [1 - 0.72 \times \exp(-0.082 \times I)]$$

where E = the kinetic energy in the shower (MJ ha^{-1} mm^{-1})

I = the shower intensity in mm hr^{-1}.

The calculation of an R factor value requires rainfall data over a long term, usually more than 20 years. In this study, a data set of 21 years was used. The EI for each year was derived and the mean value for all the years was considered to be the rainfall erosivity R factor. Seasonal and half-month rainfall erosivity values were computed using the mean values of EI over the 21 years for each half-month and season.

* Steven Hollinger is a Senior Program Scientist with the Illinois State Water Survey, Champaign, IL.

4 Methods for Spatial and Temporal Modeling

Experimental semi-variograms measuring the spatial and temporal variability of rainfall erosivity were first calculated and modeled for the large area (Fort Hood, Texas, and the surrounding states). Spatial and temporal prediction and uncertainty analysis for annual, seasonal, and half-month R factors were then done using sequential Gaussian simulation. The prediction and variance maps of the R factor values were derived over space and time. The prediction and uncertainty maps for the Fort Hood study area were extracted from those for the large area. Simulations were tested using the differences between estimates and observations from the validation data. The results were compared with those obtained using traditional isoerodent maps in terms of uncertainty analysis.

Because the rainfall stations were not systematically located in the larger study area, data for the rainfall erosivity R factor were de-clustered to obtain a reasonable weight for each station. Further, the Gaussian simulation requires normal distributions of data, so normal score transformation of the original data was done to make the transformed data normally distributed. The spatial variability of the transformed data (instead of the original data) was then modeled using semi-variograms and used in the simulations. The methods are briefly described below.

Semi-variogram

A semi-variogram measures the spatial variability of a random variable. By sampling a random variable (z) in a study area, observations (n) are acquired (z(ua) (a = 1, 2,...,n)). The vector of spatial coordinates of the a^{th} individual is ua. The experimental semi-variogram g(h) is generally calculated from samples using the following expression (Krige 1966):

Equation 2. Semi-variogram equation.

$$\gamma(h) = \frac{1}{N(h)} \sum_{\alpha=1}^{N(h)} (z(u_\alpha) - z(u_\alpha + h))^2$$

where N(h) = the number of pairs used

h = vector separating two values

z(ua) and z(ua+h) = the two values of the interest variable separated by a distance of h.

The magnitude of the semi-variogram quantifies the spatial variability. The larger the magnitude of the semi-variogram, the higher the spatial variability and the lower the spatial correlation in the data set.

Ideally, the value of the semi-variogram should be zero when the separation vector h is zero. In practice, this is usually not true because of measurement errors. In this case, a so-called "nugget effect" (nugget variance) exists. As the semi-variogram increases, separation distance increases and reaches its maximum at a distance called range parameter. The maximum semi-variogram value is sill parameter (structured variance). The experimental semi-variograms are often fit using several models that include spherical, Gaussian, and exponential models, and the model that best fits the data is selected. Additionally, different directions are taken into account to determine whether the spatial variability is isotropic or anisotropic.

Simple Kriging

Simple kriging allows the estimation of unknown locations based on information gathered from the known locations within a neighborhood given a radius for searching for the data. Kriging estimates incorporate the spatial variability structure of the data into predictions. The simple kriging estimator (Krige 1966) is given as:

Equation 3. Simple kriging estimator equation.

$$Z^*_{sk}(u) = \sum_{\alpha=1}^{n(u)} \lambda^{sk}_{\alpha}(u) Z(u_{\alpha}) + \left[1 - \sum_{\alpha=1}^{n(u)} \lambda^{sk}_{\alpha}(u)\right] m$$

where $Z^*_{sk}(u)$ = a simple kriging estimate at an unknown location (u)

n(u) = the number of the data used at the known locations given a neighborhood

$\lambda^{sk}_{\alpha}(u)$ = the weight assigned to the datum z(ua)

m = the expectation value of Z(u).

In simple kriging, the mean should be a known constant over all the area. The error variance is minimized under the constraints that it is unbiased with an error mean of zero. The error variance, σ_{sk}^2, is usually written in terms of covariance functions, C(.) (Goovaerts 1997), and it is:

Equation 4. Error variance equation.

$$\sigma_{sk}^2 = C(0) - \sum_{\alpha=1}^{n(u)} \lambda_\alpha^{sk}(u) C(u_\alpha - u)$$

Sequential Gaussian Simulation

Sequential Gaussian simulation assumes that the underlying distribution is Gaussian. As such, the appropriateness of the data distribution must thus be tested before simulation. Distribution that is not normal requires a normal score transformation of the original data into a new data set with a standard normal cumulative density function, and then the simulated values need to be transformed back to the original scale.

A data set $\{z(u_\alpha), \alpha = 1,2,3,...,n\}$ is sampled from a study area divided into N nodes where $\{Z(u_j'), j = 1,2,3,...,N\}$ is a set of random variables defined at N locations $\{u_j'\}$. Conditionally, L joint realizations $\{z^{(l)}(u_j'), j = 1,...,N\}$ exist for l = 1, 2, ..., L. The N random variables can be generated in the sequential Gaussian simulation. The N-point conditional cumulative density function is expressed as the product of N one-point conditional cumulative density functions given the set of n original data values and N-1 realizations (Goovaerts 1997). If $F(u_N'; z_N \mid (n+N-1))$ is the conditional cumulative density function of $Z(u_N')$ given the set of n original data values and the N-1 previous realizations $Z(u_j') = z^{(l)}(u_j'), j = 1,...,N-1$, the N-point conditional cumulative density function follows:

Equation 5. Cumulative density function.

$$\begin{aligned} F(u_1',...,u_N'; z_1,...,z_N \mid (n)) = {} & F(u_N'; z_N \mid (n+N-1)) \times \\ & F(u_{N-1}'; z_{N-1} \mid (n+N-2)) \times ... \times \\ & F(u_2'; z_2 \mid (n+1)) \times F(u; z_1 \mid (n)) \end{aligned}$$

The steps for the simulation are:

1. Test the appropriateness of multi-Gaussian distribution by declustering and performing normal score transformation of the original data and developing standardization semi-variograms.
2. Define a random path to visit each node of the grid only once in the study area.
3. At the first node to be visited, calculate the mean and variance of the Gaussian conditional cumulative density function given the n original data using simple kriging and the modeled normal score semi-variogram. From the conditional distribution above, draw a value, transform it back to the original data, and add it to the data set.
4. At the i^{th} node to be visited, determine the parameters of the Gaussian distribution given the n original data and all (i-1) simulated values at the locations previously visited, and for the i^{th} node. From that conditional distribution draw a value that is transformed back and becomes a conditional datum for all subsequent drawings.
5. Repeat step 4 until all N nodes are visited and provided with simulated values.

Running L times, each time with a possible different path to the N nodes, will lead to L realizations from which an expected value and prediction variance for each node can be derived. The realizations thus provide a visual measure and a model of spatial uncertainty.

As previously mentioned, simple kriging estimates are smoothed and are best in local prediction; however, kriging variances depend only on the data configuration and not on the actual observed data, and thus do not adequately reflect uncertainty. The advantage of the sequential Gaussian method over kriging methods is that it provides spatial uncertainty analysis by calculating conditional variances. The conditional variance depends on not only data configuration but also on data values. This conditional variance in theory will provide a more realistic assessment of uncertainty across space.

5 Results

Spatial and temporal variation of annual and seasonal rainfall erosivity R factor observations for the large area are shown in Figure 2. The annual and seasonal R factor values were lower at the west, increased from the west to the central east, and slightly decreased further to the east. The annual R factor values increased slightly from the north to the central and then decreased slightly to the south. Winter, spring, and autumn R factor values increase slightly from the north to the south, and the summer values decreased slightly along the direction of the north to south. Overall, the summer R factor values were the largest, followed by autumn, spring, and winter R factor values, which were the smallest. The Fort Hood study area had no rainfall stations; however, there were four stations in the proximity of Fort Hood. Their annual rainfall erosivity R factor values varied from 317 to 392.

The observations of half-month rainfall R factor values are not presented here because of space limitations. The spatial variability of the observations for each half-month map was similar to that of the annual and seasonal ones in Figure 2. That is, the largest values were distributed at the central east and the smallest at the west, but their spatial variability was more smooth compared with that of annual and seasonal R factor values. The half-month R factor values and their spatial variability rose slowly from the first half of January to the second half of March, then rose rapidly until the first half of June. After that period, they began a trend of very slight decrease and fluctuation until the first half of October, then decreased until December. The smallest values and variability occurred in the first half of January and the largest occurred in the first half of June.

Figure 3 shows an example comparison of the data distribution with and without normal score transformation. The distribution of original data was obviously not normal. The transformation led to a new data set that was normally distributed. The spatial variability of annual, seasonal, and half-month R factor values were then analyzed by experimental semi-variograms in the directions of azimuth 0, 45, 90, and 135 degrees. The semi-variograms were similar at all the directions and considered isotropic. Figure 4 shows an example of isotropic semi-variograms.

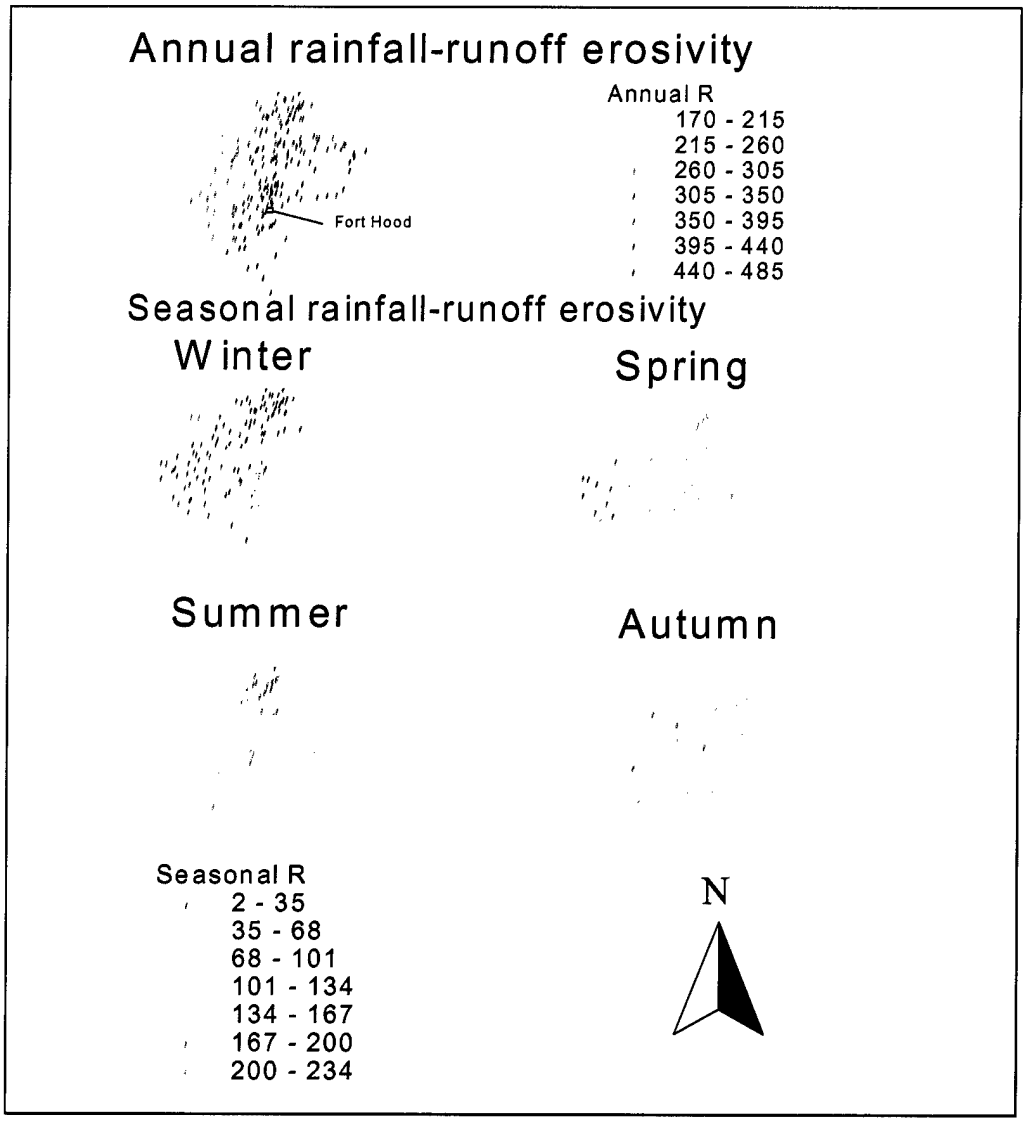

Figure 2. Spatial location of rainfall stations in the large area used for calibration and their annual (top right) and seasonal rainfall erosivity R factor (bottom left).

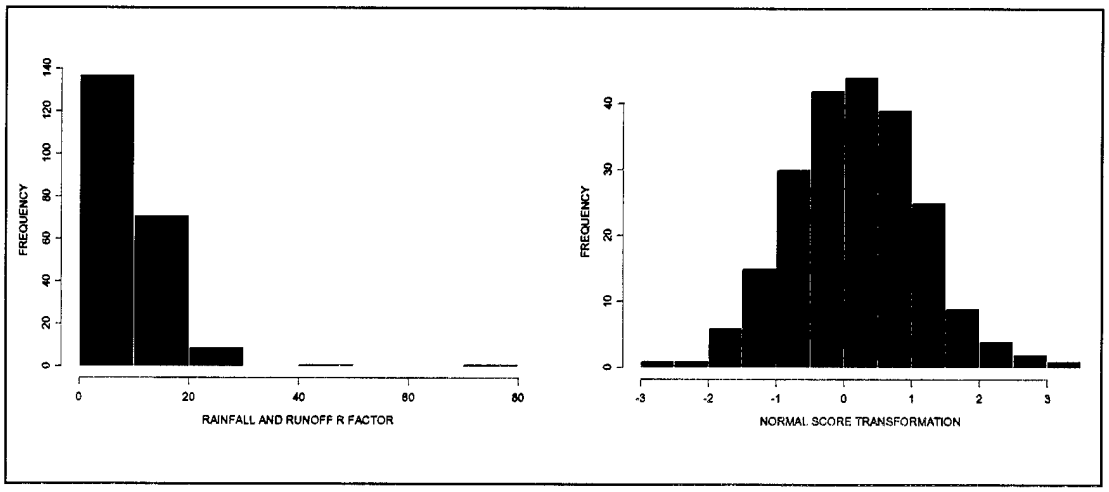

Figure 3. Comparison of data distribution without (left) and with (right) normal score transformation for the rainfall erosivity R factor for the second half of September.

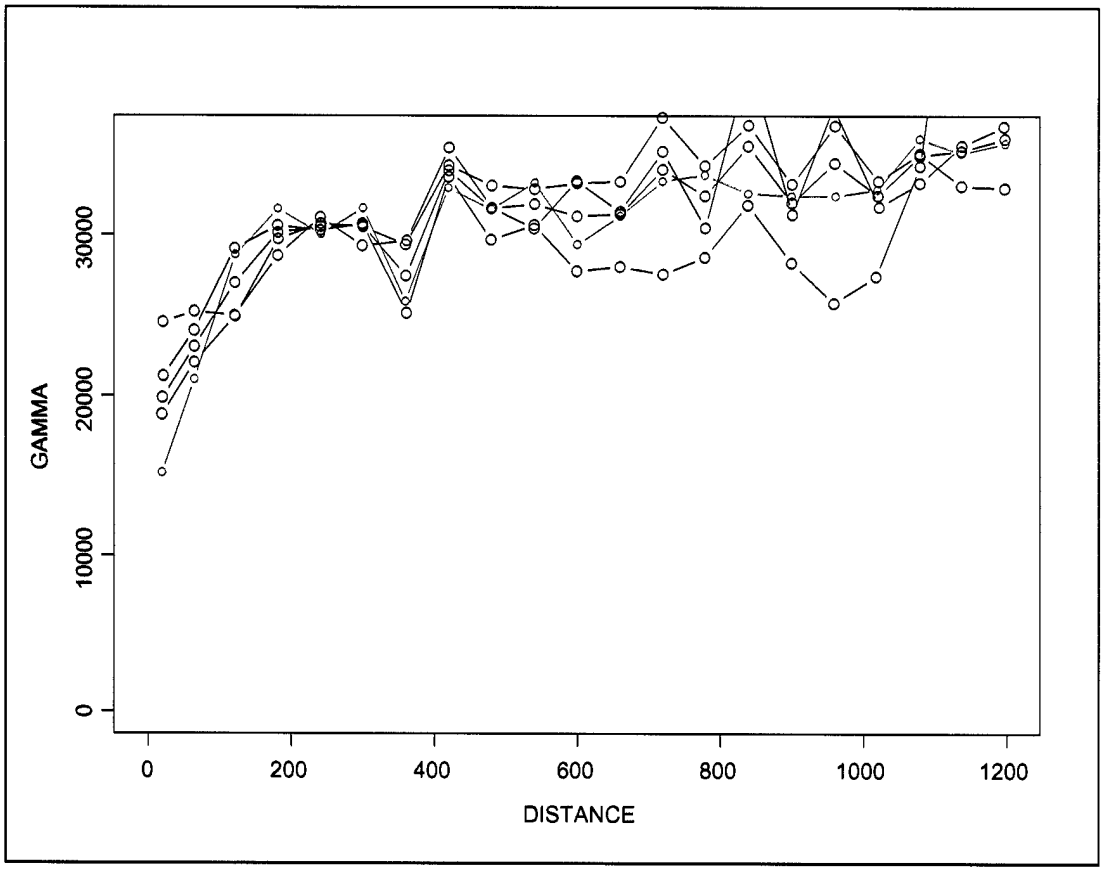

Figure 4. An illustration of the examining isotropic feature of experimental semi-variograms for four directions (00, 450, 900, and 1350) for the rainfall R factor during the second half of September.

The experimental and modeled semi-variogram of annual R factor values using the original data is shown in Figure 5. The Gaussian model was the best semi-variogram model in terms of fit for the original data. Figure 6 shows experimental and modeled semi-variograms of seasonal rainfall R factor values using the original data. The Gaussian model was also found to best fit the semi-variograms. With the normal score transformation and standardization, the semi-variograms for annual and seasonal rainfall R factor values were further modeled. Their nugget, sill, and range parameters are in Table 2, together with those parameters using the original data. After standardization, the sum of sill and nugget was forced to be one unit. The experimental and modeled semi-variograms for half-month rainfall R factor values were developed. The figures and model parameters are omitted here because of space limitation. A total of 24 semi-variogram models were obtained, including 17 Gaussian, 6 spherical, and 1 exponential models.

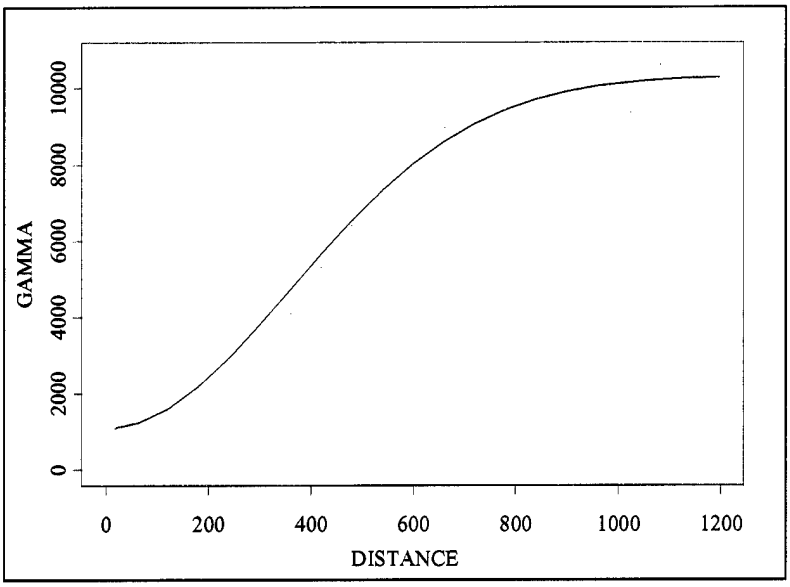

Figure 5. Experimental (dots) and modeled (line) omni-directional semi-variogram for annual rainfall erosivity R factor values.

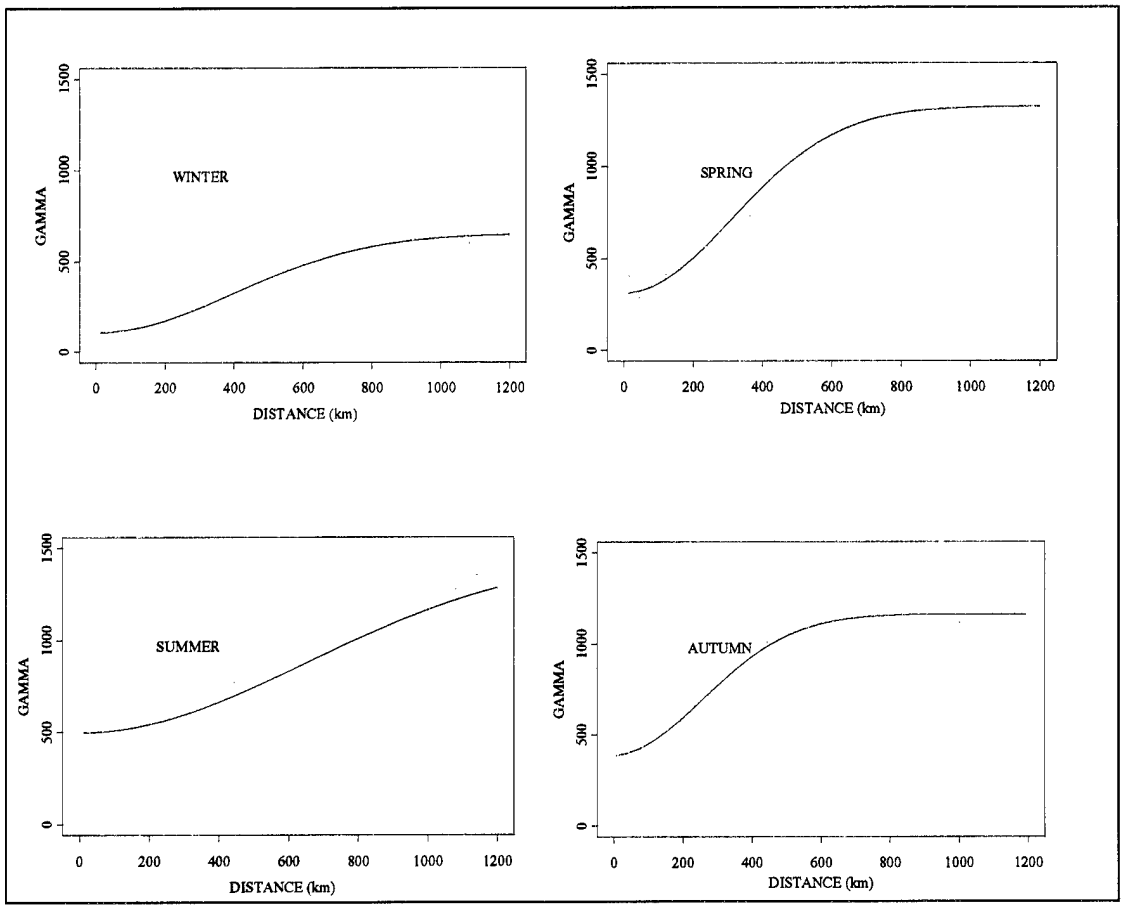

Figure 6. Experimental (dots) and modeled (line) omni-directional semi-variograms for seasonal rainfall erosivity R factor values.

Table 2. Parameters of semi-variograms using original and standardized data.

Rainfall R factor	Original data (nonstandardized)				Normal score data (standardized)			
	Nugget	Sill	Range	Model	Nugget	Sill	Range	Model
Annual	1085.6	9233.6	508.7	G	0.353	0.647	827.9	G
Winter	106.6	543.6	558.5	G	0.150	0.850	900.0	S
Spring	310.8	1011.9	435.8	G	0.300	0.700	1000.0	S
Summer	496.3	965.1	920.3	G	0.400	0.600	800.0	S
Autumn	375.1	775.9	369.8	G	0.350	0.650	1200.0	S

Note: G = Gaussian model; S = Spherical model

The prediction and variance maps of annual rainfall R factor values for the large area are shown in Figure 7. The predicted values of the annual R factor had similar spatial distribution to that of the observations. That is, they increased from the west to the east and from the north to south, but the highest values existed in the central east. As would be expected, the prediction variances were higher outside the area of rainfall stations. In the large area, the denser the rainfall stations, the lower the prediction variance. The lowest variances existed in the central east area because of the high density of rainfall stations. Further, variances were higher in the central west due to the lower density of rainfall stations.

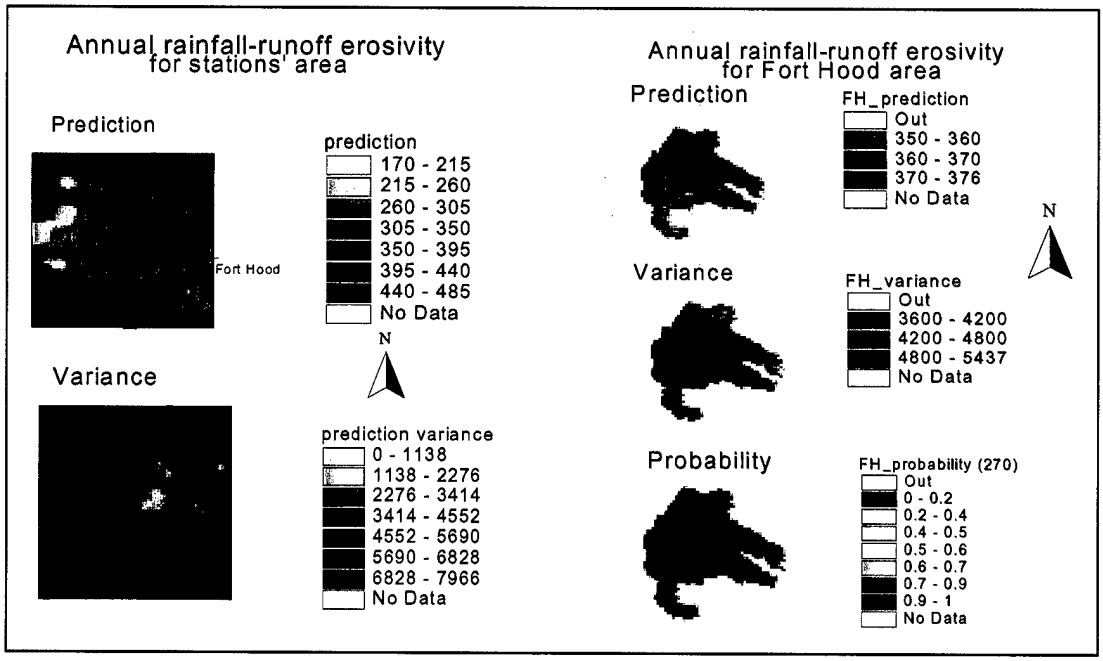

Figure 7. Prediction and variance images of annual rainfall erosivity R factor values for the large area (left) and Fort Hood (right), and the probability map for annual rainfall erosivity being larger than 270 (bottom right).

The prediction and variance maps for the Fort Hood area were then extracted from the corresponding maps for the large area and are shown at the right in Figure 6. The figure also shows the probability map for the annual R factor value larger than 270 at Fort Hood. The predicted values varied from 350 to 376. The estimates were not a constant over space, however, and much higher than 270 derived from the commonly used isoerodent map for Fort Hood. The probabilities of all the predicted values larger than 270 were higher than 0.7. The variances of the predicted values ranged from 3600 to 5437.

Figure 8 shows the results of spatial and temporal prediction and uncertainty analysis for seasonal rainfall erosivity R factor values for both the large area and the Fort Hood area. The predicted values in the large area (Figure 8, upper left) varied over space and time. The values were consistent with observations of the seasonal R factor values in Figure 2. The lowest prediction was in the west and the largest in the central east. Winter, spring, and autumn prediction values slightly increased from the north to the central and slightly decreased from the central to the south. For the summer, high prediction values were in some localized areas in the north and south. Over the four seasons, the summer had the largest predicted values and the winter had the lowest. The predicted values in spring and autumn were similar.

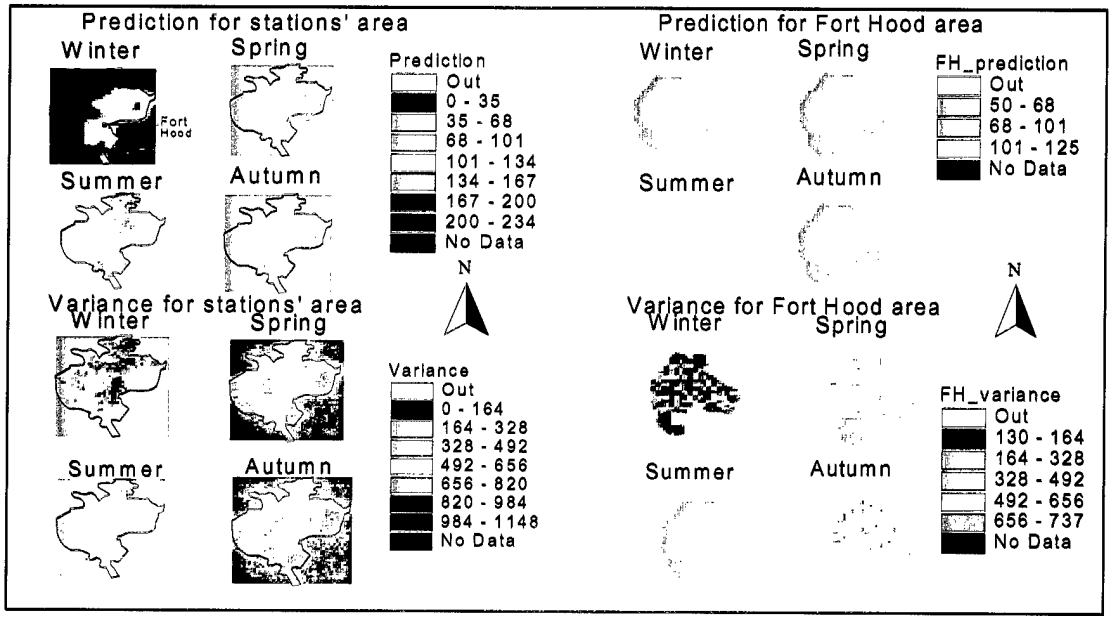

Figure 8. Prediction (top) and variance (bottom) images of seasonal rainfall erosivity R factor values for the large area (left) and Fort Hood area (right).

The variances of the predicted values in spring and autumn, however, were larger than those in winter and summer (Figure 8, lower left). The winter R factor values had the smallest prediction variances. As with the annual R factor values, the prediction variances were higher outside of the rainfall stations' area. Within the rainfall stations' area, the sparser the rainfall stations and the higher the spatial variability of seasonal R factor values, the larger the prediction variances. These features for the large area could also be applied to the seasonal prediction and variance maps for the Fort Hood area (Figure 8, right). The estimates and their variances were more smoothing, however, because Fort Hood is only a small area within the model development region.

Figure 9 shows the 24 prediction maps produced from the spatial and temporal predictions for half-month rainfall erosivity R factor values for the large area. The predicted R factor values had similar spatial and temporal distributions to those of the corresponding observations. Generally, the largest values were at the central east and the smallest were at the west. The spatial variability, however, was more smoothing than that in the annual and seasonal prediction maps. The predicted half-month R factor values varied from 0 to 85. Overall, the values increased slowly over the first six half-months and rapidly until the first half of June. The values then fluctuated and decreased slightly until October; then quickly decreased to December.

From the large area maps in Figure 9, 24 prediction maps of half-month rainfall R factor values for Fort Hood area were extracted and are presented in Figure 10. The predicted values varied from 0 to 31.5 and had less spatial variability compared with those for the whole area. They rose from the first half of January to the first half of June, then decreased up to December. Fluctuations occurred in some months (e.g., the second half of March had higher values than the first half of April, and the second half of December had larger values than the first half of December). From the second half of June to the second half of October, the temporal variability of the predicted values was relatively small.

The prediction variance images of half-month rainfall-runoff erosivity R factor values for the large area were created but are not shown here. As observed in spatial variability of the original observations, the variances increased overall from January to June, then decreased up to December except for the time from the second half of September and the first half of October, in which the variances were greater than those in August and the first half of September. The largest variances occurred in the first half of June. The 24 variance maps for the Fort Hood area (Figure 11) were extracted from the corresponding prediction variance maps for the large area. The variances changed from 0 to 233. When the predicted values were small and their spatial variabilities low, their uncertainty in

terms of variances was low. When the predicted values were large and their spatial variabilities high, their uncertainty in terms of variances was high. The first half of January, for example, had the smallest variances because of small rainfall R factor values, and the first half of June had the greatest variances because of large R factor values.

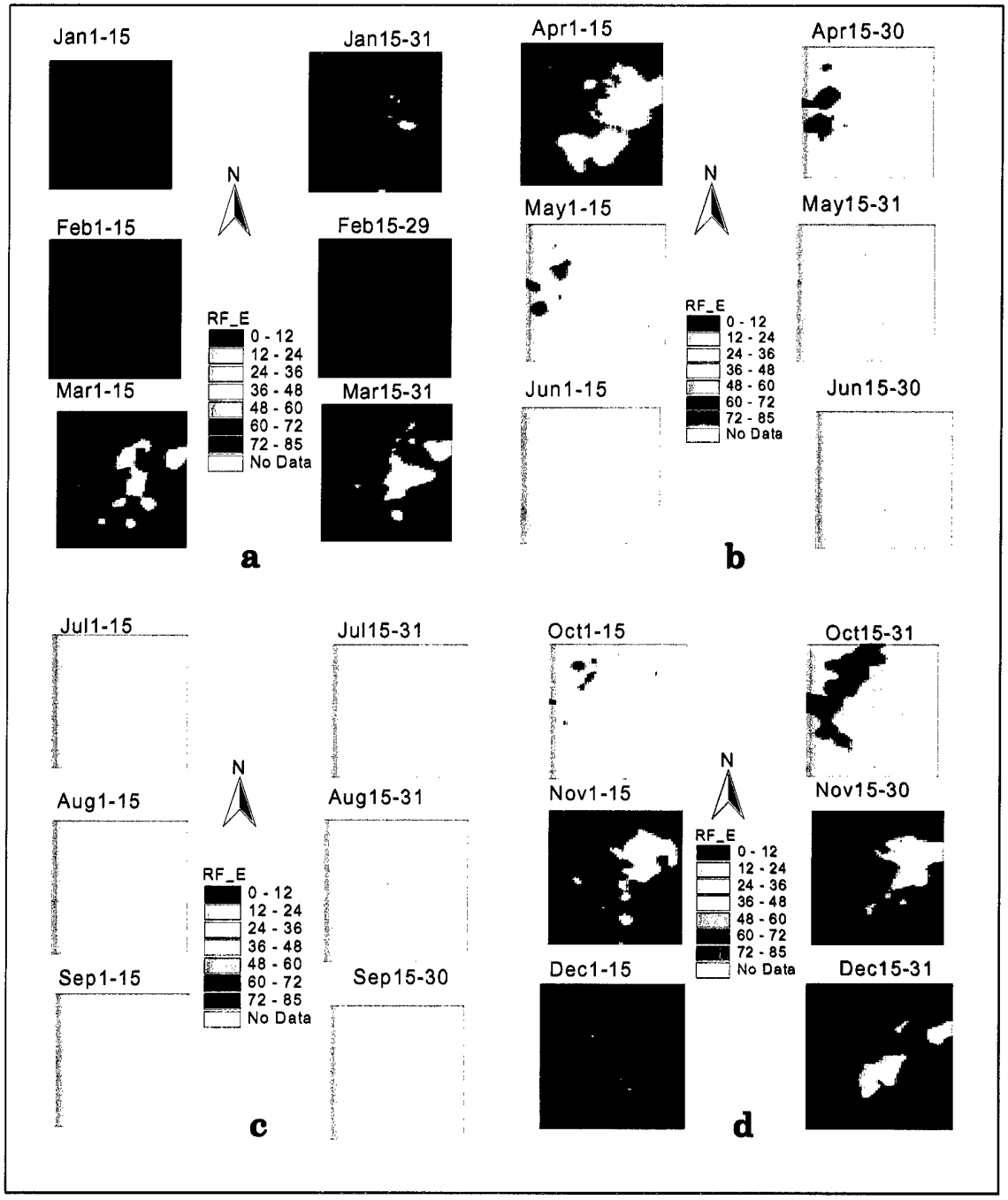

Figure 9. Prediction images of rainfall erosivity R factor values, on a half-month basis over the large area where the rainfall stations are located.

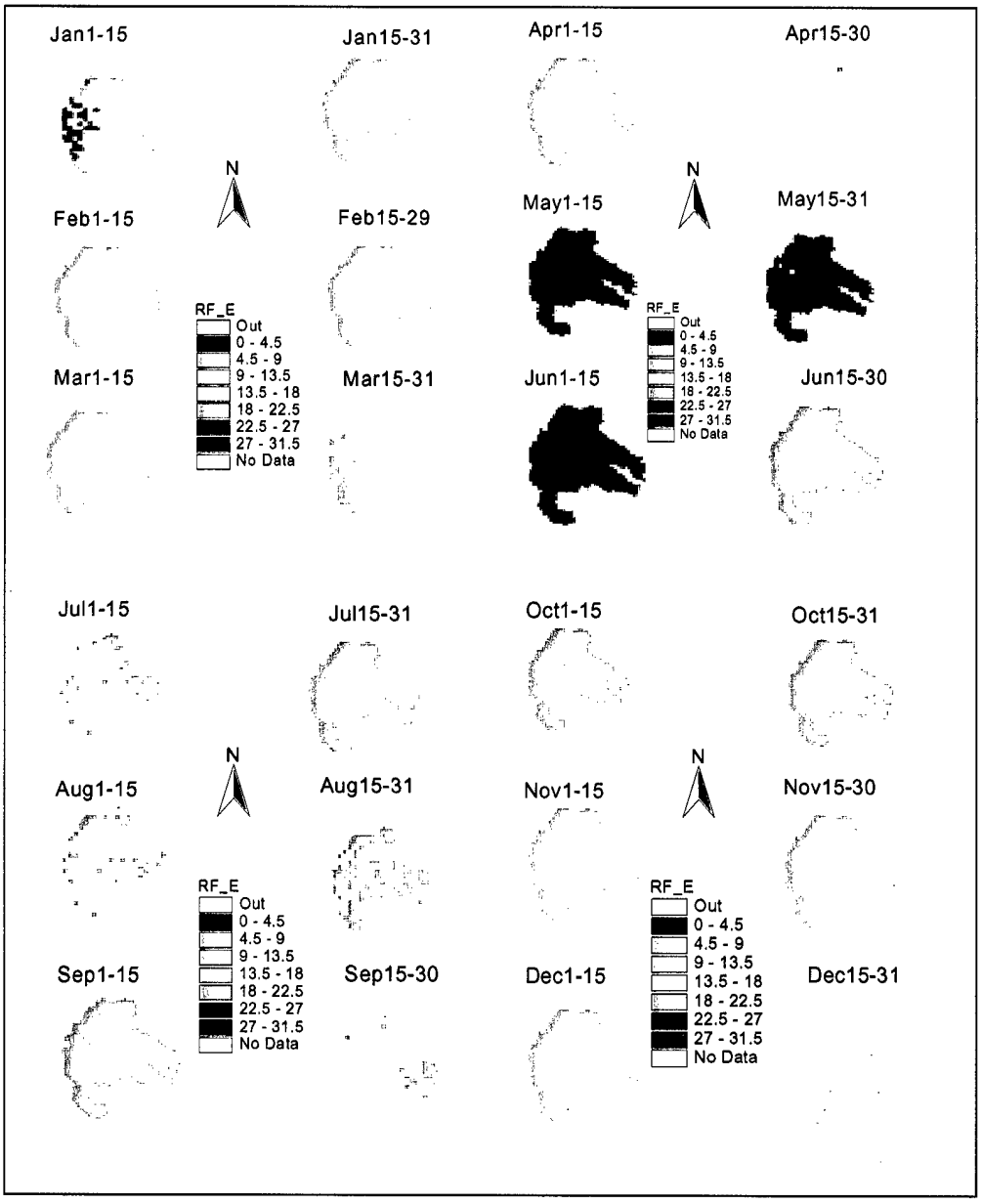

Figure 10. Prediction images of half-month rainfall erosivity R factor values in the Fort Hood area.

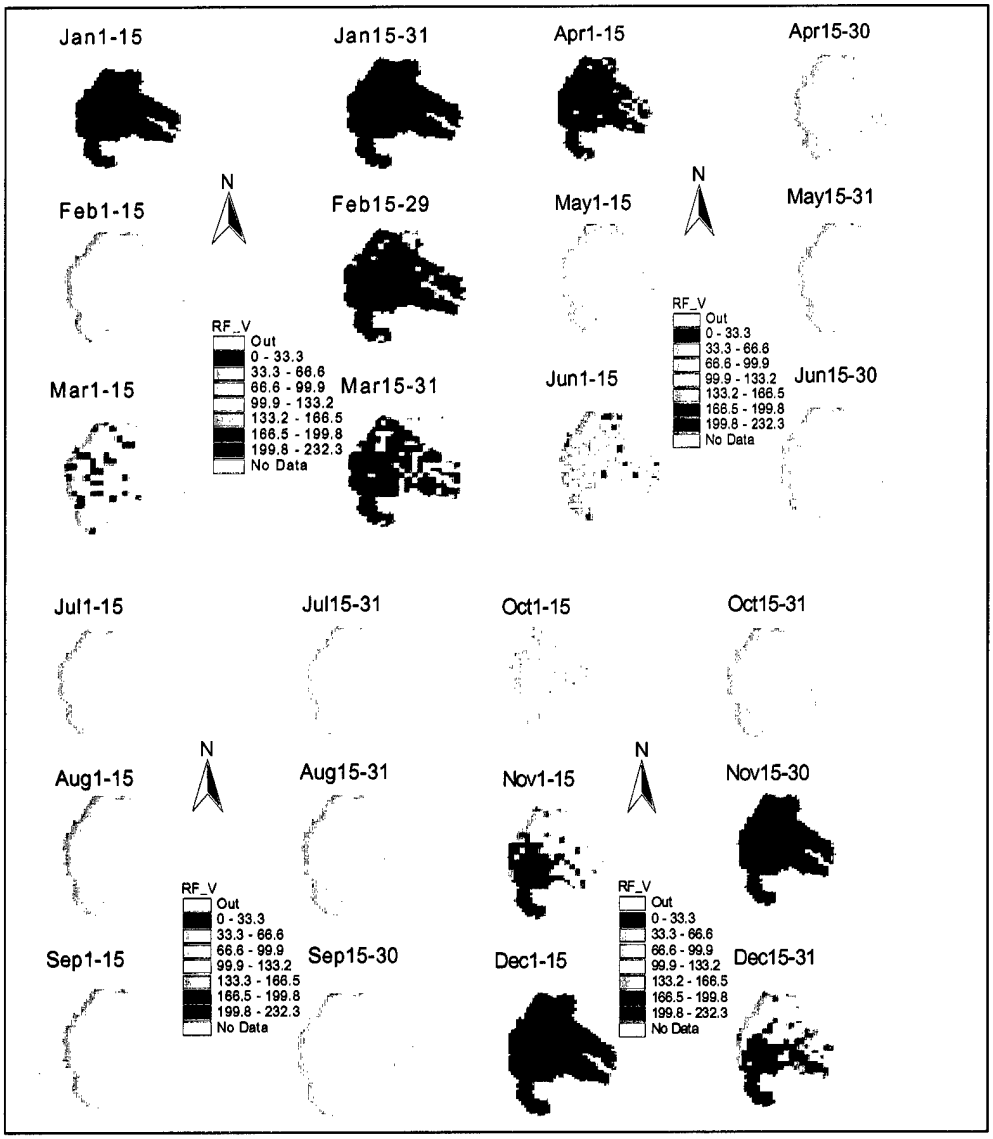

Figure 11. Prediction variance images of half-month rainfall erosivity R factor values for the Fort Hood area.

The differences between the predicted and observed R factor values for annual rainfall erosivity were calculated and plotted against observations using the test data of 29 rainfall stations (Figure 12). The observations varied from 190 to 465, and the differences obtained using the simulation varied from -120 to 120. Overestimation occurred in the areas with lower R factor values and underestimation in the areas with higher R factor values. According to coordinates of 30 rainfall stations, the rainfall erosivity R factor values were obtained by the traditional method of interpolating the isoerodent map and also comparing the observations shown in Figure 12. The differences fell in the range of 0 to -250. The underestimation occurred for all the rainfall stations and was much worse in direction and amount than the occurrence of underestimation and overestimation by the simulation.

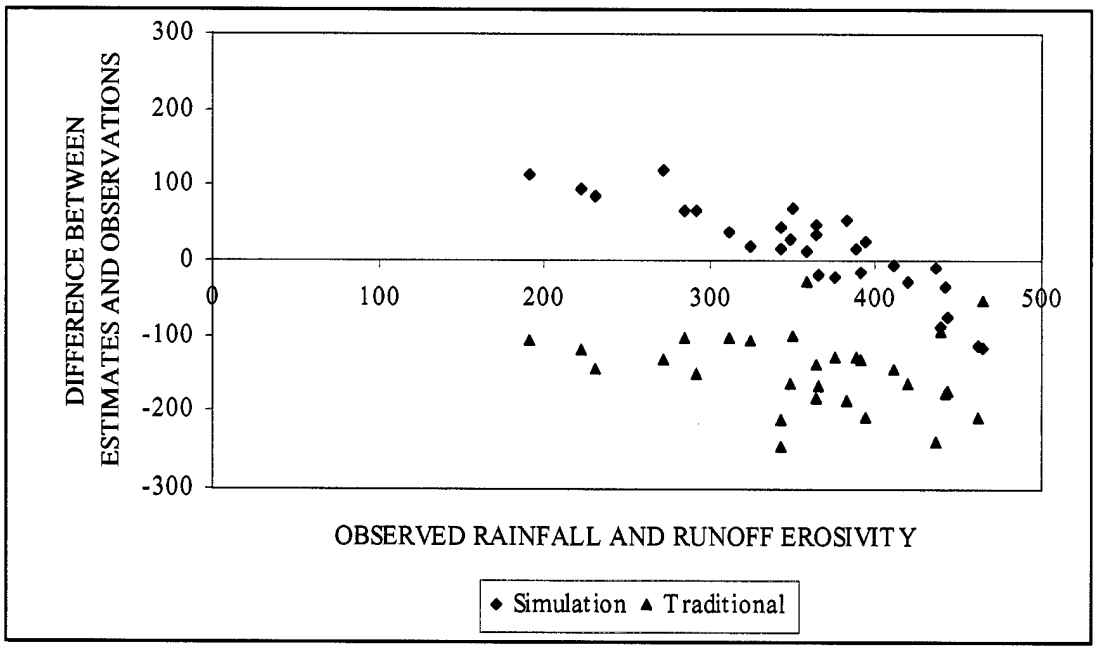

Figure 12. Difference between estimate and observation errors versus observed annual rainfall erosivity R factor values for the large area using simulation and a traditional isoerodent map.

The simulation also resulted in over- and underestimations to the seasonal predictions in Figure 13 and the overestimation was slightly more significant than underestimation. The range of relative errors (the ratio of a difference to an observation) for the seasonal R factor values was the smallest in summer, followed by autumn, spring, and winter, although the absolute errors were smaller in winter than in other seasons.

The error analysis used the test data of 29 rainfall stations for the annual and seasonal rainfall erosivity R factor values (Table 3). Overall, the simulation for annual R factor values led to the average estimate falling into the confidential interval at the significant level of 5 percent, although it was slightly overestimated. The traditional method of using an isoerodent map resulted in serious underestimation with a large and negative mean difference and an average estimate out of the confidential interval. The root mean square error (RMSE) using the isoerodent map was 251 percent of that using the simulation. In Table 3, the average estimates for summer and spring rainfall R factor values were within the confidence intervals at the significant level of 5 percent, and the corresponding average estimates for winter and autumn were very close to the upper limit of the confidential interval.

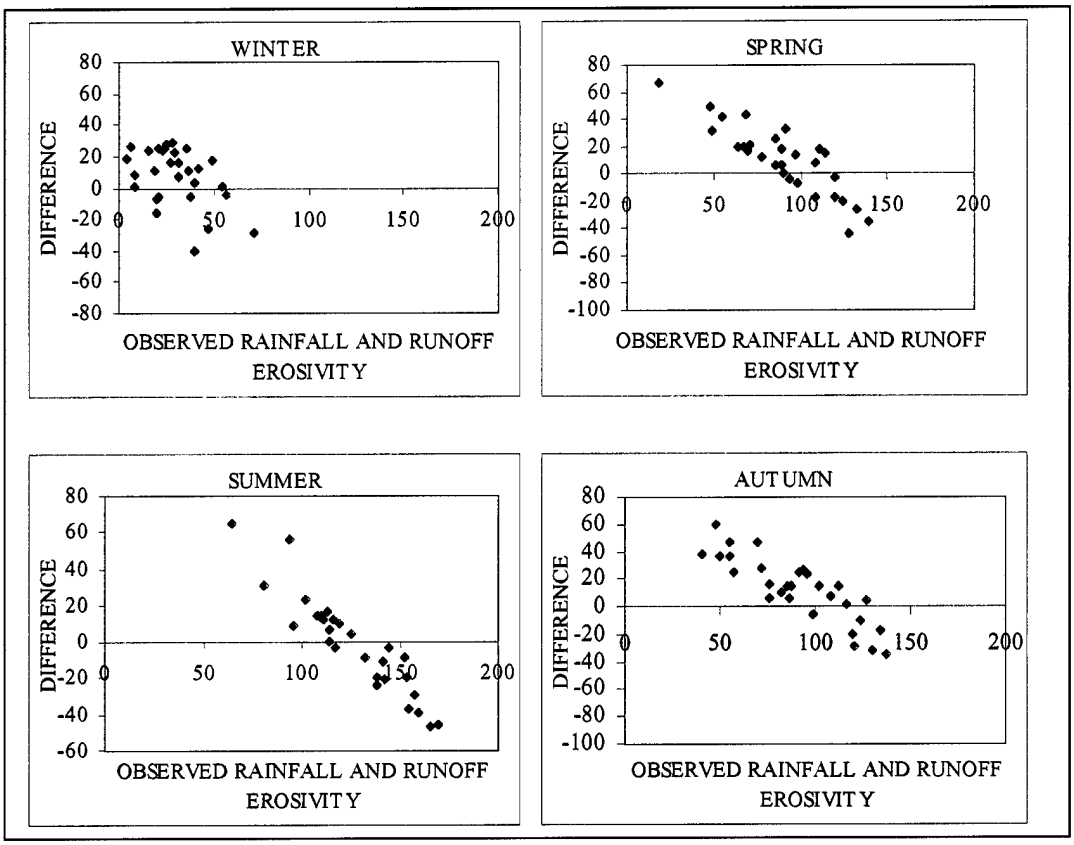

Figure 13. Difference between estimates and observations versus observed seasonal rainfall erosivity R factor values for the large area using the simulation.

Table 3. Error analysis for predicting annual and seasonal rainfall erosivity R factor values using the test data from 29 observations.

R factor	Mean of Test Data	Stdv of Test Data	Confidential Interval		Mean of Estimates	Difference	RMSE
			Lower	Upper			
Annual	359.06	71.60	331.60	386.66	373.34**	14.28**	61.93**
					212.17*	-146.9*	155.24*
Winter	30.04	16.02	23.87	36.22	37.37	7.33	19.35
Spring	90.19	28.64	79.15	101.23	100.22	10.02	26.88
Summer	127.22	26.40	117.04	137.40	125.12	-2.10	26.55
Autumn	91.54	28.42	80.59	102.50	103.81	12.27	26.65

Note: Stdv = standard deviation, RMSE = root mean square error, the significant level is 5 percent, * = traditional method, and ** = simulation.

The estimates and observations for time series of half-month rainfall R factor values were compared using the test data in Figure 14. All the average estimates fell within the confidential intervals and were very close to their mean observations. The differences between the estimated and observed values fluctuated around zero from -2.4 to 1.8. The maximum RMSE existed in the first half of October and March, when the largest variation of the rainfall R factor was observed in the test data.

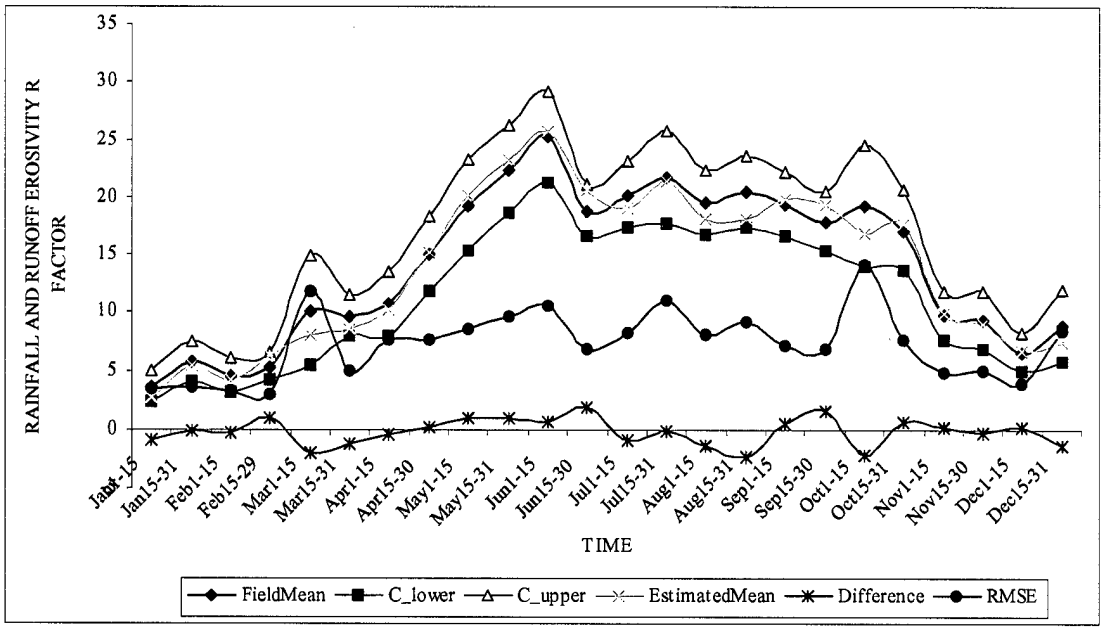

Figure 14. Difference and RMSE between estimates and observations; mean of estimates (EstimatedMean) of rainfall erosivity R factor values over half-months compared with field mean (FieldMean); and lower and upper limits of the confidential intervals (C lower and C upper) of observed values.

6 Conclusions

The sequential Gaussian simulation strategy reported in this study provided the spatially and temporally predicted values and their uncertainty measures in terms of prediction variances for rainfall erosivity R factor values in predicting soil loss at unknown locations and areas. The spatial and temporal distributions of the predicted values were similar to the observed data from the rainfall stations. This method reproduced the variability of the data over space and time, and can thus be recommended as a monitoring and mapping strategy for spatial and temporal prediction and uncertainty analysis of the rainfall erosivity R factor in predicting soil loss. The results also provide important inputs required to complete an overall uncertainty analysis of the RUSLE.

The rainfall erosivity R factor is an important variable in the prediction of soil loss. However, it is difficult to derive the R factor values in areas where no rainfall stations exist. Traditionally, the most widely used method is to interpolate the R factor values from the isoerodent maps where R factor values are assumed constant over time. The method presented in this report suggested a possible improvement over the traditional approach in deriving the R factor values.

In fact, the results from the validation data showed that all the average estimates of the R factor by the simulation for annual, seasons, and half-months were within the confidential intervals, except that winter and autumn data were very close to the upper limit. The average estimate of annual rainfall R factor values by the isoerodent map was outside its corresponding interval and systematically negative. The annual rainfall R factor values obtained by the simulation for the Fort Hood areas without any rainfall stations varied from 350 to 376, falling into the R factor values of four rainfall stations around it, but much higher than the R factor of 270, which was based on the isoerodent map. That is, the annual R factor values from the traditional isoerodent map for the large and small areas were much less than the observed and simulated values, which is consistent with the findings by McGregor, Mutchler, and Bowie (1980). The reason for the lower traditional values may be, in part, because different equations and data sets were used for calculation of the R factor values for each rainfall station.

The results in this study also implied that the annual rainfall erosivity R factor had a large variability over space. Even within a relatively small area, such as Fort Hood with an area of 87,890 ha, the spatial variability may not be overlooked. Moreover, there was a high temporal variability of the R factor in the time series of seasons and half-months. As expected, the summer had the largest R factor values, then autumn, spring, and winter. The half-month rainfall R factor values increased from January to June, then fluctuated and decreased slowly to October, and after that tended to rapidly decrease to December. These findings indicate a necessity to derive the local estimates and their uncertainties in both space and time for the soil loss prediction system in which spatial and temporal variability cannot be overlooked. On the other hand, these findings also imply an importance of vegetation cover to reduce soil loss in summer by reducing water runoff.

When an isoerodent map is used to estimate the rainfall R factor value, its uncertainty is unknown. The simulation method reported here provides estimates with variances at any unknown locations. Where the rainfall stations used for model development were dense and the rainfall R factor value was low, small variances resulted; otherwise the variances were large. Decisionmakers can therefore apply the rainfall R factor estimates based on careful assessment of their uncertainties.

References

Anderson, A.B. 1999. *Sensitivity Analysis of the Army Training and Testing Area Carrying Capacity (ATTACC) Model to User-specified Starting Parameters.* CERL Technical Report 99/64/ADA367756, Department of the Army, Construction Engineering Research Laboratory (CERL), Champaign, IL.

Anderson, A.B., L. Chenkin, L. Winters, R. Hunt, C. Couvillon, D. McFerren, S. Sekscienski, and P. Sydelko. 1996. "Evaluation of Land Value Study (ELVS)/Army Training and Testing Area Carrying Capacity (ATTACC)." In *5th Annual LRAM/ITAM Workshop Proceedings.* August 27-29, 1996. LaCrosse, WI, pp 8-17.

Army Regulation (AR) 350-4, *Integrated Training Area Management (ITAM),* 8 May 1998.

Bollinne, A., A. Laurant, P. Rosseau, J.M. Pauwels, D. Gabriels, and J. Aelterman. 1980. "Provisional rain erosivity map of Belgium." In M. DeBoodt and D. Gabriels (ed.), *Assessment of Erosion.* John Wiley & Sons, pp 111-120.

Concepts Analysis Agency. 1996. *Evaluation of Land Value Study (ELVS).* U.S. Army Concepts Analysis Agency, Study Report CAA-SR-96-5, Bethesda, Maryland.

Council on Environmental Quality. 1989. *Defense Lands and Installations.* Environmental Quality: Annual Report, 1987-88. Washington, DC.

Department of the Army Pamphlet (DA PAM) 350-4, *Facilities Engineering and Housing Annual Summary of Operations, Fiscal Year 1987: Volume III – Installations Performance* (Office of the Assistant Chief of Engineers, Washington, DC, 1987).

Deutsch, C.V. and A.G. Journel. 1998. Geostatistical software library and user's guide. Oxford University Press, Inc.

Goovaerts, P. 1999. "Using elevation to aid the geostatistical mapping of rainfall erosivity." *Catena,* 34: 227-242.

Goovaerts, P. 1997. *Geostatistics for Natural Resources Evaluation.* Oxford University Press, Inc.

Gould, F.W. 1975. *Texas Plants—A Checklist and Ecological Summary,* MP-585/Rev. (Texas A&M University, Texas Agricultural Experiment Station, College Station, TX).

Juang, K.W. and D.Y. Lee. 1998. "A comparison of three kriging methods using auxiliary variables in heavy metal contaminated soils." *J. Environ. Qual.* 27:355-363.

Krige, D.G. 1966. "Two-dimensional weighted moving average trend surfaces for ore evaluation." *Journal of the South African Institute of Mining and Metallurgy.* 66: 13-38.

McGregor, K.C., C.K. Mutchler, and A.J. Bowie. 1980. Annual R values in North Mississippi. *J. of Soil and Water Conservation*. March-April 1980:81-84.

Mikhailova, E.A., R.B. Bryant, S.J. Schwager, and S.D. Smith. 1997. Predicting rainfall erosivity in Honduras. *Soil Sci. Soc. Am. J.* 61:273-279.

Nakata Planning Group, Inc., *Master Plan Report: Fort Hood, Texas* (U.S. Army Corps of Engineers, Fort Worth, TX, 1987).

Public Land Law Review Commission. 1970. "One third of the Nation's Land." A report to the President and to the Congress. U.S. Government Printing Office, Washington, DC.

Renard, K.G., C.R. Foster, G.A. Weesies, D.K. McCool, and D.C. Yoder. 1997. *Predicting soil erosion by water: A guide to conservation planning with the Revised Universal Soil Loss Equation* (RUSLE). U.S. Department of Agriculture, Agriculture Handbook Number 703. Government Printing Office, Washington, DC.

Rogowski, A.S. and J.K. Wolf. 1994. "Incorporating variability into soil map unit delineations." *J. Soil Sci. Soc. Am.* 58:163-174.

U.S. Army Environmental Center (AEC), *ATTACC Handbook* (AEC, 1999). http://www.army-itam.com/main.htm

Wang, G., G. Gertner, P. Parysow, and A.B. Anderson. 2000. Spatial prediction and uncertainty analysis of topographical factors for the Revised Universal Soil Loss Equation (RUSLE). *Journal of Soil and Water Conservation* 55:3:374-384.

Wischmeier, W.H. 1959. A rainfall erosion index for a universal soil loss equation. *Soil Sci. Soc. Am. Proc.* 23:246-249.

Wischmeier, W.H. and D.D. Smith. 1978. Predicting rainfall-erosion losses from cropland east of the Rocky Mountains: Guide for selection of practices for soil and water conservation. U.S. Dep. Agric., Agric. Handbook No. 282.

Wischmeier, W.H. and D.D. Smith. 1958. "Rainfall energy and its relationship to soil loss." *Trans. AGU* 39:285-291.

CERL Distribution

Chief of Engineers
ATTN: CEHEC-IM-LH (2)

Army Headquarters
ATTN: DAMO-TRO
ATTN: SFIM-AEC-ECN
ATTN: ATIC-CTS

Engineer Research and Development Center (Libraries)
ATTN: ERDC, Vicksburg, MS
ATTN: Cold Regions Research, Hanover, NH
ATTN: Topographic Engineering Center, Alexandria, VA

Defense Tech Info Center 22304
ATTN: DTIC-O

SERDP (2)

11
3/01

REPORT DOCUMENTATION PAGE

Form Approved
OMB No. 0704-0188

1. REPORT DATE (DD-MM-YYYY)	2. REPORT TYPE	3. DATES COVERED (From - To)
05-2001	Final	

4. TITLE AND SUBTITLE
Spatial and Temporal Prediction and Uncertainty Analysis of Rainfall Erosivity for the Revised Universal Soil Loss Equation

5a. CONTRACT NUMBER

5b. GRANT NUMBER

5c. PROGRAM ELEMENT NUMBER

6. AUTHOR(S)
Guangxing Wang, George Gertner, Vivek Singh, Svetlana Shinkareva, Pablo Parysow, and Alan B. Anderson

5d. PROJECT NUMBER
SERDP

5e. TASK NUMBER

5f. WORK UNIT NUMBER
EE9

7. PERFORMING ORGANIZATION NAME(S) AND ADDRESS(ES)
U.S. Army Engineer Research and Development Center (ERDC)
Construction Engineering Research Laboratory (CERL)
P.O. Box 9005
Champaign, IL 61826-9005

8. PERFORMING ORGANIZATION REPORT NUMBER
ERDC/CERL TR-01-39

9. SPONSORING / MONITORING AGENCY NAME(S) AND ADDRESS(ES)
Strategic Environmental Research and Development Program
901 N. Stuart St., Suite 303
Arlington, VA 22203-1853

10. SPONSOR/MONITOR'S ACRONYM(S)

11. SPONSOR/MONITOR'S REPORT NUMBER(S)

12. DISTRIBUTION / AVAILABILITY STATEMENT
Approved for public release; distribution is unlimited.

13. SUPPLEMENTARY NOTES
Copies are available from the National Technical Information Service, 5285 Port Royal Road, Springfield, VA 22161.

14. ABSTRACT

Prediction of soil loss is important when a sustainable environment is expected. The Revised Universal Soil Loss Equation (RUSLE) is widely used to predict longtime average annual soil loss based on rainfall, soil erodibility, slope length and steepness, cover management, and support practice. The rainfall erosivity R factor, defined as the sum of erosivity index values for all rain events in one year, best indicates soil loss due to rainfall. The larger the R factor value, the more the soil loss. In previous military applications, the R factor value, obtained from empirical isoerodent maps, is assumed constant over time. At the same time, it is considered linear and smooth over space. For a specific area, a constant is usually applied. Recent studies suggest, however, that those assumptions may not hold and may result in uncertainty both temporally and spatially in terms of predicting R factor values. This report proposes a strategy for prediction and uncertainty analysis of this factor. The temporal and spatial variability of the R factor is first modeled using semi-variograms in geostatistics. Its prediction and uncertainty analysis is then carried out using sequential Gaussian simulation. The strategy is illustrated in a case study at Fort Hood, TX. Additionally, the report assesses the uncertainty caused by traditional applications of isoerodent maps. The results are also important for overall uncertainty analysis of RUSLE.

15. SUBJECT TERMS
Army Training and Testing Area Carrying Capacity (ATTACC) | training lands | land management
Integrated Training Area Management (ITAM) | SERDP | military training | carrying capacity

16. SECURITY CLASSIFICATION OF:			17. LIMITATION OF ABSTRACT	18. NUMBER OF PAGES	19a. NAME OF RESPONSIBLE PERSON
a. REPORT	b. ABSTRACT	c. THIS PAGE			Alan B. Anderson
Unclassified	Unclassified	Unclassified	SAR	38	19b. TELEPHONE NUMBER (include area code) (217) 373-6390